Recombinant human bone morphogenetic protein 6 delivered within autologous blood coagulum restores critical size segmental defects of ulna in rabbits

Grgurević, Lovorka; Oppermann, Hermann; Pećin, Marko; Erjavec, Igor; Capak, Hrvoje; Pauk, Martina; Karlović, Sven; Kufner, Vera; Lipar, Marija; Bubić Špoljar, Jadranka; ...

Source / Izvornik: **JBMR Plus, 2018, 3**

Journal article, Published version
Rad u časopisu, Objavljena verzija rada (izdavačev PDF)

https://doi.org/10.1002/jbm4.10085

Permanent link / Trajna poveznica: https://urn.nsk.hr/urn:nbn:hr:105:915117

JBMR PLUS Open Access ASBMR

Recombinant Human Bone Morphogenetic Protein 6 Delivered Within Autologous Blood Coagulum Restores Critical Size Segmental Defects of Ulna in Rabbits

Lovorka Grgurevic,[1] Hermann Oppermann,[2] Marko Pecin,[3] Igor Erjavec,[1] Hrvoje Capak,[4] Martina Pauk,[1] Sven Karlovic,[5] Vera Kufner,[1] Marija Lipar,[3] Jadranka Bubic Spoljar,[1] Tatjana Bordukalo-Niksic,[1] Drazen Maticic,[3] Mihaela Peric,[1] Reinhard Windhager,[6] T Kuber Sampath,[7] and Slobodan Vukicevic[1]

[1]Laboratory for Mineralized Tissues, School of Medicine, University of Zagreb, Zagreb, Croatia
[2]Genera Research, Kalinovica, Sveta Nedelja, Croatia
[3]Clinics for Surgery, Orthopedics, and Ophthalmology, School of Veterinary Medicine, University of Zagreb, Zagreb, Croatia
[4]Department of Radiology, School of Veterinary Medicine, University of Zagreb, Zagreb, Croatia
[5]Faculty of Food Technology and Biotechnology, University of Zagreb, Zagreb, Croatia
[6]Department of Orthopedics and Trauma Surgery, Medical University of Vienna, Vienna, Austria
[7]perForm Biologics Inc., Holliston, MA, USA

ABSTRACT

BMP2 and BMP7, which use bovine Achilles tendon–derived absorbable collagen sponge and bovine bone collagen as scaffold, respectively, have been approved as bone graft substitutes for orthopedic and dental indications. Here, we describe an osteoinductive autologous bone graft substitute (ABGS) that contains recombinant human BMP6 (rhBMP6) dispersed within autologous blood coagulum (ABC) scaffold. The ABGS is created as an injectable or implantable coagulum gel with rhBMP6 binding tightly to plasma proteins within fibrin meshwork, as examined by dot-blot assays, and is released slowly as an intact protein over 6 to 8 days, as assessed by ELISA. The biological activity of ABGS was examined in vivo in rats (*Rattus norvegicus*) and rabbits (*Oryctolagus cuniculus*). In a rat subcutaneous implant assay, ABGS induced endochondral bone formation, as observed by histology and micro-CT analyses. In the rabbit ulna segmental defect model, a reproducible and robust bone formation with complete bridging and restoration of the defect was observed, which is dose dependent, as determined by radiographs, micro-CT, and histological analyses. In ABGS, ABC scaffold provides a permissive environment for bone induction and contributes to the use of lower doses of rhBMP6 compared with BMP7 in bovine bone collagen as scaffold. The newly formed bone undergoes remodeling and establishes cortices uniformly that is restricted to implant site by bridging with host bone. In summary, ABC carrier containing rhBMP6 may serve as an osteoinductive autologous bone graft substitute for several orthopedic applications that include delayed and nonunion fractures, anterior and posterior lumbar interbody fusion, trauma, and nonunions associated with neurofibromatosis type I.

KEY WORDS: BONE MORPHOGENETIC PROTEIN 6; AUTOLOGOUS BLOOD COAGULUM CARRIER; CRITICAL SIZE DEFECT; AUTOLOGOUS BONE GRAFT SUBSTITUTE; FRACTURE HEALING

Introduction

Bone heals spontaneously upon fracture by recapitulating the cellular events associated with embryonic bone development,[1–3] except when compromised by smoking, use of steroids, pseudoarthrosis in NF-1 patients, and osteoporosis.[1,4,5] The large bone defects caused by tumors, trauma, congenital disorders, and infection also fail to heal and over time become a nonunion representing challenging issues in orthopedic medicine and a burden for the health care system.[1,6] In approximately 10% of cases, bone fractures heal slowly or fail to heal and require additional medical interventions.[7,8] For example, tibial nonunion can potentially lead to the loss of the function or even loss of limb.[9] The medical need in this clinical area warrants new and effective therapies to be developed and introduced in clinical practice.

Autograft is a gold standard to promote bone healing and restore function for segmental long bone defects, delayed and nonunion fractures, and spinal fusion procedures. The availability of autologous bone tissue, limited in quantity and morbidity, is associated with harvested site, which demands an alternative to autograft bone.[10–12] Allogenic demineralized bone matrix (DBM) has been used widely as an option to induce new bone formation because it provides osteoinductive signals and

Received in original form June 28, 2018; revised form August 29, 2018; accepted September 16, 2018. Accepted manuscript online November 05, 2018.
Address correspondence to: Slobodan Vukicevic, MD, PhD, Laboratory for Mineralized Tissues, School of Medicine, University of Zagreb, Salata 11, HR-10000 Zagreb, Croatia. E-mail: slobodan.vukicevic@mef.hr

JBMR® Plus (WOA), Vol. 3, No. 5, May 2019, e10085.
DOI: 10.1002/jbm4.10085

osteoconductive substratum.[13–15] Advances made in the isolation of bone morphogenetic proteins (BMP) from DBM[16] and subsequently the identification of the corresponding genes[17,18] allowed the production of recombinant human BMPs in promoting fracture healing at compromised settings.[19–21] Recombinant BMP2 soaked in absorbable collagen sponge (InFuse) and recombinant BMP7 combined with bovine bone collagen (OP1-Putty) have been approved as biologic bone graft substitutes to bridge the gap and restore delayed and nonunion fractures.[22–24]

BMP alone cannot form bone unless it is delivered with an appropriate scaffold and responding cells are available in a permissive environment.[25–30] Studies thus far have used animal-derived collagens as scaffold for BMP2 and BMP7 in approved products and collagens, synthetic calcium phosphate-based ceramics, and precalcified cellulose matrix as scaffolds in preclinical studies.[31–33] In clinical studies, rhBMP2 containing collagen has been used in reconstruction of mandibular bone defects[34,35] and delayed diaphysis fractures. Evaluation of rhBMP2 containing ceramic-collagen composite device in posterolateral lumbar fusion (PLF), however, has not met primary endpoint and failed to get an FDA approval. This device was also reported to have unwanted side effects likely attributed to the use of a high dose of rhBMP2 and its weak binding to collagen-ceramics.[6,36–38]

Here we describe an autologous bone graft substitute (ABGS) that is composed of recombinant human BMP6 (rhBMP6) combined with autologous blood coagulum (ABC) to guide the formation of new bone to promote bone healing in a large diaphysis segmental defect and bridge the gap. ABC circumvents the use of animal-derived collagen, limiting possible inflammatory processes due to its autologous nature, provides functional and physiological carrier for rhBMP6, and offers a flexibility to mold to the desired shape, thus facilitating its use within different anatomical structures.[9] We also describe the method of formulation using ABC and rhBMP6, binding and release characteristics of rhBMP6 from plasma proteins, and rheological properties for in vivo bone-inducing activity in rat subcutaneous implants and rabbit critical size ulna defect.[39] The preclinical data generated represent a solid foundation to progress the ABGS toward further stages of drug development and its use in human orthopedic indications.

Materials and Methods

Recombinant human BMPs

The manufacturing process for rhBMP6 was developed and is conducted by Genera Research (Kalinovica, Croatia). Engineered Chinese Hamster Ovary (CHO) cell line was used to produce and purify rhBMP6 from the media using heparin affinity and hydrophobic interaction chromatography, followed by the reverse phase HPLC. It was then lyophilized and stored at $-20°C$ in vials containing 0.5 mg $>99\%$ pure rhBMP6. rhBMP2 and rhBMP7 used in in vitro experiments were from R&D Systems (Abingdon, UK). rhBMP7 for in vivo experiments was used as OP-1 Putty commercial device (Ossigraft) for human use.

Mouse C2C12-BRE-Luc reporter gene assay

The activity of rhBMP6 was determined in mouse C2C12-BRE-Luc BMP reporter cell assay, stably transfected with a reporter plasmid consisting of a BMP response element (BRE) from the Id-1 promoter fused to a luciferase reporter gene (kindly provided by Dr Gareth Inman).[40] To measure the luciferase activity, 20 μL of the cell lysate was added to 100 μL luciferase assay reagent (Promega, Madison, WI, USA) and luminescence was then quantified by Wallac Victor luminometer (PerkinElmer, Waltham, MA, USA).

Formulation of rhBMP6 within ABC

Blood samples were collected from rabbit marginal ear veins into tubes without anticoagulant substance in a volume of 1.5 mL. rhBMP6 was added into the blood in the amounts of 25 μg, 50 μg, and 100 μg with 50 mM concentration of calcium chloride and mixed by rotating the tubes. ABC + rhBMP6 were prepared in a syringe and left at room temperature to coagulate for 60 to 90 minutes. The liquid portion (serum) was removed and the homogeneous, cohesive, injectable and malleable ABGS gel was ready for use.

rhBMP6 characterization and release studies

For rhBMP6 identification and characterization, lyophilized protein samples were subjected to SDS-PAGE electrophoresis, transferred to the nitrocellulose membrane, and analyzed by Western blot using the rhBMP6-specific monoclonal antibody (available in the rhBMP6 DuoSet ELISA kit, R&D Systems, DY507). To demonstrate rhBMP6 stability in the coagulum after ABGS formation, ABGS was homogenized 60 and 90 minutes after preparation in 2% SDS, insoluble particles were removed by centrifugation, and supernatants were analyzed by Western blot using the same rhBMP6-specific antibody.

For determination of the release profile of rhBMP6 from the ABGS, rhBMP6 was added to the blood in two concentrations, 2 and 5 μg/mL. After the coagulum was formed, it was placed in the basal medium and the release profile of the rhBMP6 was determined during a period of 14 days. The medium was changed every 2 days, and samples of medium for rhBMP6 measurement were collected on days 1, 3, 5, 8, 10, and 12 after ABGS formation. rhBMP6 released into the medium was measured by the commercially available rhBMP6-specific ELISA (R&D Systems, DY 507).

Binding affinity of rhBMP6 for plasma proteins

Autologous fibrinogen concentrate (FC) was prepared from human plasma, obtained from healthy volunteers. rhBMP6 was radiolabeled with radioactive technetium (^{99m}Tc) using the IsoLink Kit Mallinckrodt (Covidien Pharmaceuticals; gift from Dr Hector H Knight). The binding affinity of ^{99m}Tc-labeled rhBMP6 to FC and other extracellular matrix (ECM) molecules, including fibrinogen, albumin, thrombin, heparan sulfate proteoglycan, collagen I and IV, as well as the retention of BMP6 in the plasma sample added into the blood before precipitation, was semiquantitatively verified.[41] Briefly, 1 mL of human blood (healthy volunteers) was drawn into a 2 mL syringe and, using a syringe connector, blood, $CaCl_2$, and 200 μL of ^{99m}Tc-rhBMP6 were mixed and left at room temperature over 90 minutes in the 2 mL syringe. After 90 minutes, each ABC was expelled from the syringe and the syringe was washed with 2 mL of 2% SDS and the wash was pooled together. Radioactivity of the samples was measured after a 2-hour incubation period using a gamma counter and was expressed as counts per minute (cpm). All values were corrected for the half-life factor of ^{99m}Tc.

Testing of ABC biomechanical parameters

For evaluation of ABC biomechanical properties, forward extrusion test (FET) and cut test were developed and validated using Texture Analyzer TA.HD Plus (Texture Technologies, Hamilton, MA, USA).[9] Sixteen samples were initiated from each individual blood sample; 8 for each of the tests. Of these, 5 were used to investigate the effect of coagulation time on ABC biomechanical properties (ie, standing at room temperature for 30, 45, 60, 75, or 90 minutes); 1 to investigate the effect of hemolysis, which was induced by vigorous shaking (tested after 60 minutes); and 2 to investigate the effect of different $CaCl_2$ concentrations (high 15 mM and low 1 mM) after 30 and 60 minutes. Overall, 9 different healthy donors (including both men [$n = 7$] and women [$n = 2$]) contributed with 15 blood samples in total. In both tests, stiffness, elasticity, and work (required for forward extrusion or cutting, respectively) were determined. The effect of time was estimated by comparing values at 30 minutes, 45 minutes, and 60 minutes to each other (30 to 60 minutes is the anticipated coagulum formation time) and by comparing values at 75 and 90 minutes to the average for 30 to 60 minutes to evaluate changes in ABGS properties after 60 minutes. The effect of blood shaking (hemolysis) was estimated by comparing the properties with and without vigorous shaking at 60 minutes. Evaluation of time effect and the $CaCl_2$ effect included multiple comparisons. The effect of $CaCl_2$ was estimated by comparing time-averaged values between coagula formed with 0 (no), 1 (low), or 15 (high) mM $CaCl_2$. General linear mixed models were fitted using SAS 9.3 (SAS Institute, Cary, NC, USA).

Animal models

The number of rats in s.c. bone formation assays was determined based on a well-known ectopic bone formation cascade in time, as previously described.[16,42] The number of rabbits per experimental group was determined by well-characterized percent of CSD bone repair in time, as previously described.[39] In brief, using general linear mixed models (GLMMs) with restricted maximum likelihood (REML) estimation to produce time-averaged difference between groups and with using four repeated assessments and assuming variability around 20% at each time point, autocorrelation 0.6, and autoregressive covariance structure, 7 animals per group per time point provide 80% power to detect such a difference at a two-sided $\alpha = 0.05$. Because there was no healing of the defect in the control animals (variability = 0%), we applied the 3R principle and decreased the number of animals to 5 per each dose group with a possibility of gradually increasing the number of rabbits up to 7 per group, if applicable.

Rat subcutaneous implant assay

Assay was performed on 12-week-old male Sprague Dawley laboratory rats (body weight 320 to 350 g). Laboratory animals were housed in polysulfonic cages in conventional laboratory conditions at 20°C to 24°C, relative humidity of 40% to 70%, and noise level 60 dB. Standard GLP diet and fresh water was provided *ad libitum*, without environmental enrichment. Animal care was in compliance with SOPs of animal facility; the European convention for the protection of vertebrate animals used for experimental and other scientific purposes (ETS 123).

rhBMP6 osteogenic activity was tested at different doses in the rat subcutaneous assay, as previously described.[16,42] ABC was prepared from 0.5 mL of rat full blood, which was mixed with an appropriate amount of rhBMP6 and left for 60 minutes to coagulate in a 1 mL syringe. After removing the serum, 370 μL of the ABGS was implanted. The osteogenic response of rhBMP6 doses (2.5 μg, 5 μg, 10 μg, and 20 μg per mL blood) was tested in two rats for each dose, as previously described.[14,43] Briefly, a small pocket was created under the skin in the axial regions to implant ABC prepared with rhBMP6. The ABC was implanted and sealed with a single suture to the fascia and three sutures for the skin. To analyze ectopic bone formation, animals were scanned using the 1076 micro-CT device (SkyScan, Bruker microCT, Kontich, Belgium) 14 days after implantation. Ectopic bone formation was observed in all groups of animals and was quantified by micro-CT analysis.

The neutrophil infiltration was determined using naphtol AS-D chloroacetate esterase staining (Sigma, St. Louis, MO, USA) on histological sections. Neutrophils were counted in the vicinity and inside ABGS using an ocular grid. Neutrophil accumulation was expressed as number of neutrophils per mm^2 in two implants from 4 rats at day 3 after implantation. Implants contained 20 μg rhBMP2/300 mg bovine Achilles tendon–derived absorbable collagen sponge; 20 μg rhBMP7/300 mg bovine bone collagen carrier; and 20 μg rhBMP6/300 μL ABC. In addition, neutrophil activity was determined at day 3 after implantation by myeloperoxidase activity (MPO), as previously described.[44] Implants (two from 4 rats) were extracted in 50 mM KPO_4 buffer, pH 6.0, homogenized for 10 minutes, sonicated for 5 minutes, and finally the lysate was centrifuged for 60 minutes at 20,000*g*.

The differential sensitivity to increasing concentration of Noggin was tested in C2C12 cells transfected with BRE-Luc reporter, in which rhBMP6 (5 μg) was more resistant to noggin-mediated inhibition compared with rhBMP7 (5 μg). Recombinant human Noggin was obtained courtesy of Dr Aris Economides (Regeneron Corp., Tarrytown, NY, USA).

Rabbit ulna segmental defect model

Study protocols were conducted in male laboratory rabbits (*Oryctolagus cuniculus*), New Zealand strain, 10 weeks old, with health certificate, body weight from 2.3 to 2.5 kg. Animal facility is registered by Directorate for Veterinary; reg. no. HR-POK-001. An approval for the animal studies was given by the Directorate for Veterinary and Food Safety, Ministry of Agriculture, Republic of Croatia (approval no. 525-10/0255-14-3). Rabbits were acclimated for 5 days and randomly assigned to their respective treatment group. Animals were housed by standard rabbit cages in conventional laboratory conditions at the temperature of 18°C to 22°C, relative humidity of 50% to 70%, fluorescent lighting provided illumination 12 hours per day, and noise level was 60 dB. Standard GLP diet (Mucedola srl, Milan, Italy), bedding, and environmental enrichment were available and fresh water was provided *ad libitum*. Animal care was in compliance with SOPs of registries Croatian Animal facility HR-POK-001; using 3R principle, pain and suffering were minimized during the experiment. European convention for the protection of vertebrate animals was used for experimental and other scientific purposes (ETS 123).

In the critical size ulna defect experiments, rabbits were prepared as described[14,39,45] and treated with rhBMP6 amounts to confirm previous rhBMP6 efficacy results. Briefly, after acclimatization period, enrofloxacin (10 mg/kg) was given to the animals by intramuscular injection 1 day before operation

and then 10 days after surgery. Before the surgery, blood was collected from rabbit marginal ear veins into tubes without anticoagulant substance. ABC was prepared 60 and 90 minutes before implantation from 1.5 mL of blood mixed with an appropriate volume of rhBMP6. Animals were randomly divided into four groups ($n = 5$ each): A) control, defect filled with ABC only; B) defect filled with ABC + rhBMP6 (25 μg/mL); C) defect filled with ABC + rhBMP6 (50 μg/mL); and D) defect filled with ABC + rhBMP6 (100 μg/mL). In another experiment ($n = 5$ per group), ABGS (1.5 mL ABC + rhBMP6 (100 μg/mL) was compared with collagen (150 mg) + rhBMP7 (100 μg/100 mg;) at weeks 2 and 8 after implantation.

Each animal was premedicated with a mixture of ketamine 50 mg/kg, acepramazine 1 mg/kg, and xylazine 5 mg/kg. Anesthesia was maintained using a mixture of 1% to 1.5% isoflurane and oxygen deliver by mask. A lateral incision, approximately 2.5 cm in length, was made, and the tissues overlying the ulna were dissected (skin and musculature). A segment of the ulna measuring 17 mm (large defect) was removed and the device was implanted into the defect site, with the radius left intact for mechanical stability, without use of internal or external fixation devices, as previously described.[9] Radiological images of the right forelimb were taken immediately after surgery and during 23-week bone healing period. During the experiment, there were no adverse effects. Rabbits' euthanasia was conducted after sedation, premedication of 3 mg/kg xylapane, and 20 mg/kg ketamine i.m. and administration of T61 (1 mL/kg) intrapulmonary.

Radiography

To monitor the critical size defect healing, X-rays were taken at weeks 6, 9, 13, 16, 19, and 23 after surgery. All obtained radiographs from rabbit bones were interpreted and scored using a radiographic grading score system[46,47] by a surgeon and a radiologist blinded to the treatment protocol and postoperative interval. Radiographic grading scores (from 0 to 6) were as follows: 0, no change from immediate postoperative appearance; 1, trace of radio-dense material in defects; 2, flocculent radio density with spots of calcification and no defect bridging; 3, defect bridged at least one point with material of nonuniform radio density; 4, defect bridged in medial, and lateral sides with material of uniform radio density (cut ends of cortex remain visible); 5, same as grade 3, at least one of four cortices obscured by new bone; 6, defect bridged by uniform new bone, cut ends of cortex not found.

Micro-CT quantification

In subcutaneous rat assay, bone formation was scanned in vivo after 14 days using SkyScan 1076 micro-CT device (SkyScan/Bruker) at 18 μm resolution, as previously described.[48,49] Scanning parameters were 50 kV/200 μA, 0.5 mm aluminum filter, 0.8° rotational shift throughout the 198° and frame averaging value set at 2. Obtained images were reconstructed using NRecon (Bruker) and the quantification was performed using CTAn (Bruker) software. For quantification of the medullary canal volume, the defect site was approximated and delineated manually after which parameters for bone volume (BV) and newly formed endosteal/medullary volume (MV) were calculated. 3D models of the scanned bones were obtained using CTVox (Bruker) software. Quantitative micro-CT results were analyzed by one-way ANOVA with post hoc test for linear trend.

Histology

Soft tissue free bones were fixed in 4% formalin for 2 weeks, and entire bone was embedded in plastic resin (Technovit 7200). Samples were cut at 5 μm slices with a diamond saw and stained using Masson Goldner Trichrome dye, as previously described.[50,51] Images were obtained using Olympus BX51 Epi-Fluorescence microscope.

Data analysis

Values are expressed as mean ± SEM or SD as indicated. For statistical comparison of two samples, a two-tailed Student's t test was used and $p < 0.05$ was considered significant. Two-way analysis of variance with Duncan's multiple range test was performed to determine the effect of treatment and time on biochemical and bone repair parameters. Additional specific data analyses are presented in figure legends. Analyses were performed by SAS for Windows 9.3 (SAS Institute).

Results

rhBMP6 production and biological activity

rhBMP6 was produced as a secretory dimeric protein from a stable CHO cell line generated by recombinant technology.[9,14] rhBMP6 was purified to near homogeneity (>99%) from the medium by subjecting to conventional ionic, hydrophobic, and metal-chelated chromatography with final reverse-phase C18-HPLC columns. rhBMP6 behaves as a diffused ~37 kDa in nonreduced condition and 17 kDa under reduced condition, as stained by Coomassie blue (Fig. 1*A*) and as cross-reacted species by Western blot using BMP6-specific antibody (Fig. 1*B*). BMP6-specific monoclonal antibody, which has been used for Western blot, recognizes all forms of nonreduced protein and mostly the larger form of reduced species. The biological activity of the purified rhBMP6 was assessed by using mouse C2C12-established myoblast cell line transfected with BMP Response Elements (BRE)–Luciferase (Leu) construct at varying doses (Fig. 1*C*).

rhBMP6 binding and release studies using blood coagulum

Blood samples taken randomly from 60 human subjects (referred to Department of Laboratory Diagnostics of University Hospital Center Zagreb) demonstrated that 75% of samples coagulated in 30 minutes, and 100% of samples achieved coagulation in 60 minutes from blood sampling (Fig. 2*A*). Studies with radioactive technetium (^{99m}Tc)-labeled rhBMP6 performed to evaluate the extent of rhBMP6 binding to coagulum show that more than 99% of ^{99m}Tc-rhBMP6 was retained in the coagulum at 30, 45, and 60 minutes after mixing with blood. Examination of the ratio of released/retained rhBMP6 from the blood coagulum over a 14-day period shows that it is released slowly from the coagulum with a mean residence time of approximately 5 to 7 days as determined by a specific ELISA (Fig. 2*B*). The analysis of the stability of rhBMP6 during the preparation of ABGS demonstrated no signs of degradation after 60 to 90 minutes and overall loss in syringes was around 5% as examined by Western blot (Fig. 2*C*). Studies on binding and biodistribution of rhBMP6 to blood proteins using radio-labeled rhBMP6, dot-blot, and immunoblot analysis demonstrated that more than 95% of the rhBMP6 was captured within the coagulum and sequestered to blood components like

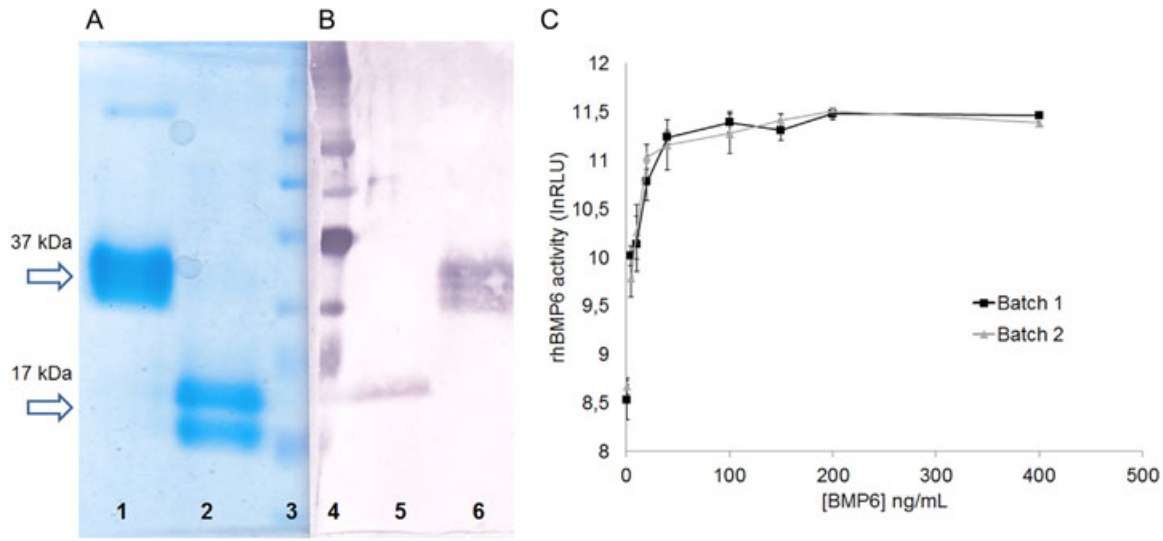

Fig. 1. Purification and biological activity of rhBMP6. SDS-PAGE analysis of rhBMP6: Coomassie-stained (*A*) and Western blot (*B*). Nonreduced (37 kDa) forms are presented in lanes 1 and 6 and reduced (17 kDa) forms are in lanes 2 and 5, respectively. Molecular weight marker (ColorBurst, Sigma-Aldrich) is indicated in lanes 3 and 4, respectively. (*C*) Specific rhBMP6 activity in C2C12-BRE-Luc reporter gene assay: comparison between two different clinical batches. The activity was tested in a range of concentrations as in *x* axis and expressed in relative light units (RLU) as in *y* axis. Data represent mean ± SEM of 3 independent measurements.

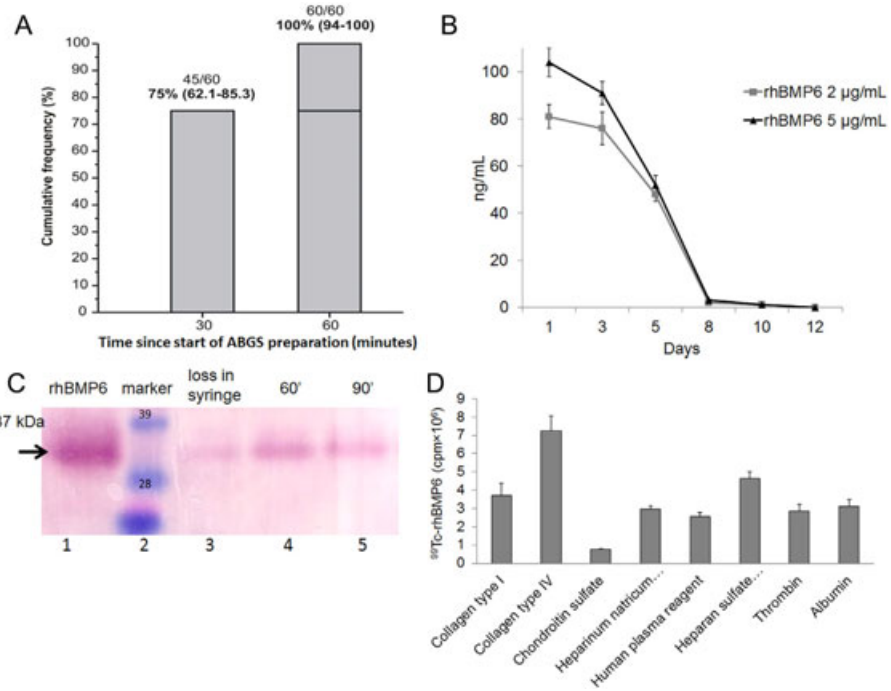

Fig. 2. Characterization of coagulation and binding, release, and stability of rhBMP6 in autologous bone graft substitute (ABGS). (*A*) Cumulative frequency of coagulation formation over time. Raw data (n/N) and percentages are shown. Bracketed values are exact 95% confidence intervals (left-sided 97.5% at 60 minutes). (*B*) Release profile of rhBMP6 from ABGS using two different concentrations of rhBMP6 over a 14-day period, as determined by ELISA. Data represent mean ± SEM of 3 independent measurements. (*C*) The stability of rhBMP6 during preparation of the ABGS implant was maintained over 60 minutes (lane 4) and 90 minutes (lane 5) with a loss of around 5% during preparation (lane 3). Arrow indicates ~35 kDa band, which corresponds to the mature rhBMP6 under nonreduced condition. (*D*) Semiquantitative analysis of ^{99m}Tc-labeled rhBMP6 binding to blood components in a dot blot assay. Mean + SEM ($n = 3$) are shown.

fibrinogen, alpha 2-macroglobulin, beta-2-microglobulin, and thrombin (Fig. 2*D*). A high level of rhBMP6 saturation (99.9%) was achieved within coagulum and the release of rhBMP6 from the coagulum within the first 24 hours was lower than 0.2%.

Examination of the time to achieve the formation of ABC consistently with defined rheological properties (stiffness, elasticity, and work load) suggests a requirement of 45 to 60 minutes (Fig. 3) to achieve a uniform coagulation, and it maintained its shape for 5 days, then reduced its size, dimension, and consistency at day 8 and dissolved by day 14. Although all the results described here are obtained using human blood samples, comparable findings were observed for rat and rabbit blood coagulum (data not shown).

Biological activity of ABGS at rat subcutaneous sites

The biological activity of ABGS was assessed in the rat subcutaneous implantation assay. The formation of endochondral bone was examined at days 1, 2, 3, 7, and 35 post-implantation by histology and micro-CT analyses. Fig. 4*A* shows the photomicrographs of ABC alone implants harvested at days 1, 3, and 7. ABC alone formed a solid pluglike implant on day 1 surrounded by a thin membrane of extracellular matrix and external mononuclear cells. Inside ABC, a layer of mesenchymal osteoprogenitor-like cells formed a zone that toward day 3 merged with external cell condensations. By day 7, the ABC showed the sign of dissolution and was replaced by normal connective tissue without evident inflammation, fibrosis, or edema, and by day 35, it completely disappeared with no sign of the implant visible. The absence of inflammatory cells and no granuloma tissue was noted. Fig. 4*B* shows the photomicrographs of ABC with rhBMP6 (25 μg/implant) implants harvested at days 1, 3, 7, and 35. Day 1 implant composed of osteoprogenitor cells (mesenchymal stem cells [MSCs]) stained positive for alkaline phosphatase. By day 3, MSCs underwent condensation with extracellular matrix expansion and sign of early chondrocytes within the "osteoprogenitor zone" slowly penetrated by cells from outside the ABC. This interconnected area of ABC composed of MSCs under the rhBMP6 influence rapidly differentiated into chondrocytes. By day 7, differentiated chondrocytes underwent hypertrophy, resulting in endochondral bone formation. By day 35, a dense trabecular bone was evident with a broad outside cortexlike structure. The cellular response elicited by ABGS (rhBMP6/ABC) was compared with rhBMP2/Bovine Absorbable Collagen Sponge and rhBMP7/Bovine Bone Collagen implants at an early time point. The

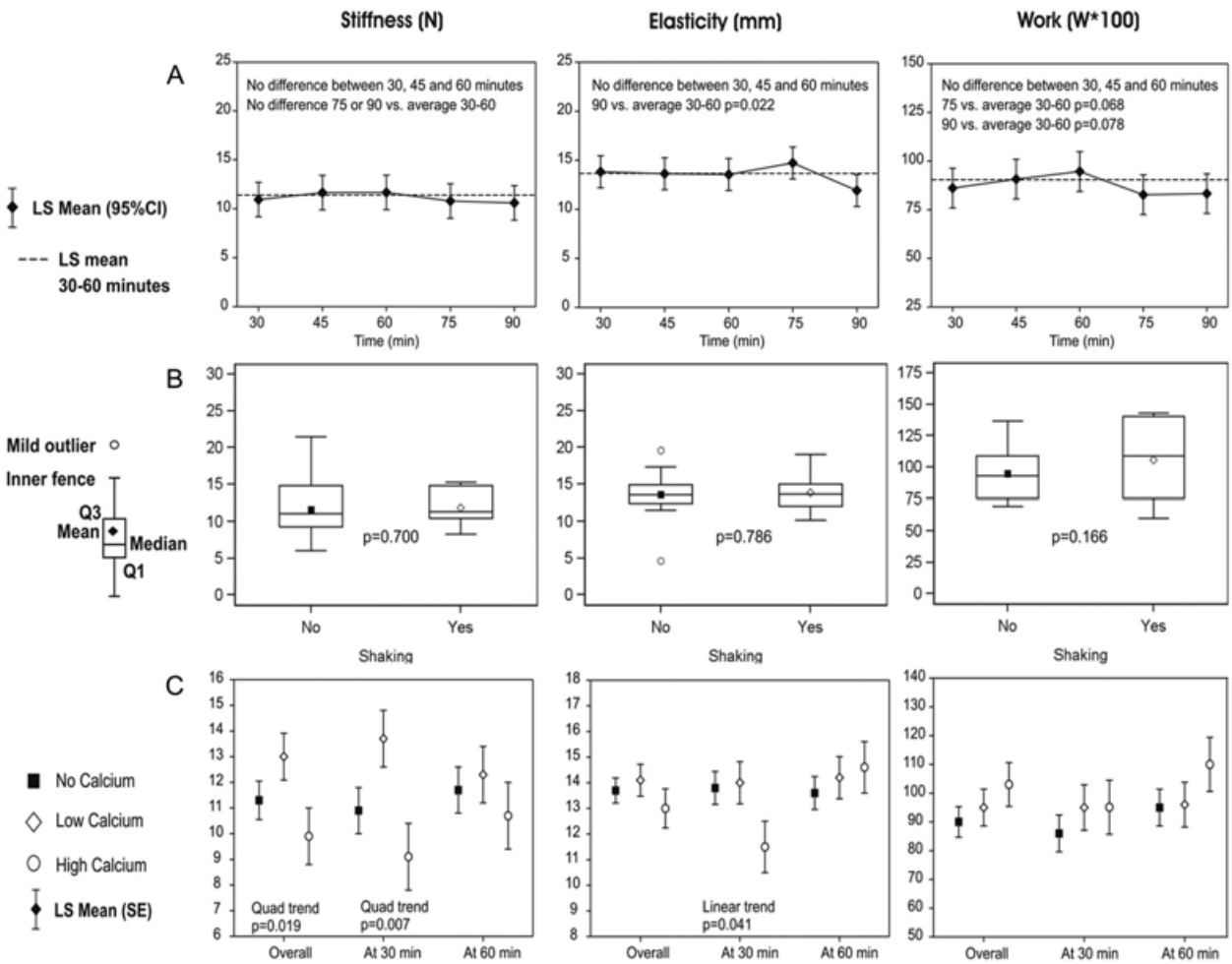

Fig. 3. Mechanical properties of the coagulum stiffness (N), elasticity (mm), and work load. (*A*) The effect of time. LS = least squares (mean). (*B*) The effect of hemolysis. $p < 0.025$ considered statistically significant (Q1, Q3–quartiles). (*C*) The effect of $CaCl_2$.

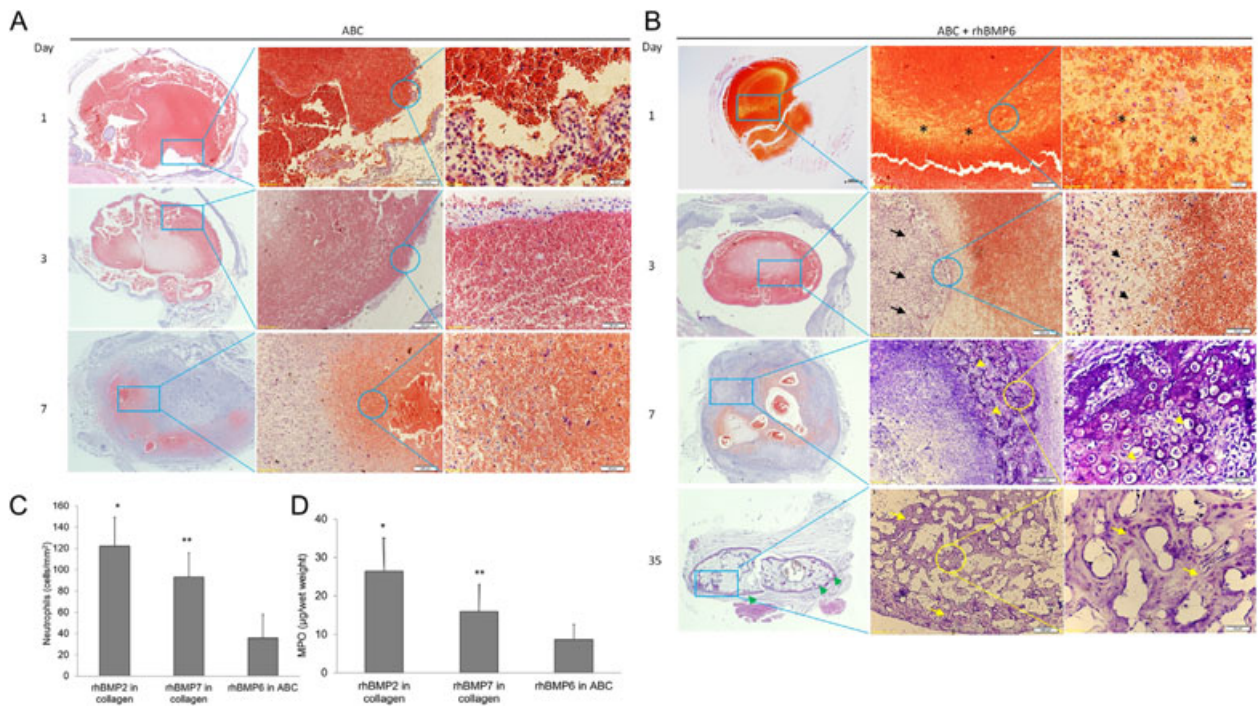

Fig. 4. Evaluation of ABGS in rat subcutaneous implants harvested at days 1, 3, 7, and 35. (*A*) Photomicrographs of histology of ABC alone at days 1, 3, and 7. Size marker: left column 500 μm (magnification 4×); middle column 200 μm (magnification 10×); right column upper (top) image 20 μm (magnification 60×) and middle and lower (bottom) image 50 μm (magnification (40×). (*B*) Photomicrographs of histology of ABGS (25 μg rhBMP6 per implant) at days 1, 3, 7, and 35. Size marker: left column 500 μm (magnification 4×); middle column upper (top) and lower (bottom) image 200 μm (magnification 10×), middle images 500 μm and 200 μm (magnification 4× and 10×, respectively); right column upper (top) image 20 μm (magnification 60×) and middle and lower (bottom) images 50 μm (magnification 40×). Asterisks denote clearly demarcated zone composed of osteoprogenitor cells stained positive for alkaline phosphatase on day 1; with condensations of extracellular matrix (black arrows) and formation of early chondrocytes within the osteoprogenitor zone (black arrowheads). On day 3, cells from outside the ABC slowly penetrated and hypertrophic chondrocytes in endochondral bone formation appeared on day 7 (yellow arrowheads). On day 35, dense trabecular bone (yellow arrows) with a broad cortexlike structure from outside demonstrated a solid persistent bone ossicle (green arrowhead). (*C*) The neutrophil infiltration on histological sections. The implants were examined on day 3 after implantation of 20 μg rhBMP2/300 mg bovine Achilles tendon, 20 μg rhBMP7/300 mg bovine bone collagen carrier, or 20 μg rhBMP6/300 μL ABC, respectively. Mean ± SEM ($n = 10$), $^{*}p < 0.01$ versus rhBMP6, $^{**}p < 0.05$ versus rhBMP6. (*D*) Myeloperoxidase (MPO) activity. Mean ± SEM ($n = 8$), $^{*}p < 0.01$ versus rhBMP6, $^{**}p < 0.05$ versus rhBMP6.

degree of inflammation, as determined by neutrophil accumulation and myeloperoxidase activity (MPO), on day 3 implants suggests that ABGS had a reduced neutrophil accumulation (Fig. 4*C*) and a lower total MPO activity (Fig. 4*D*) compared with BMP2- or BMP7-containing xenogeneic collagen implants. Macroscopically, visualization after removal of implants from the rat's axilla is shown in Fig. 5*A* and indicates absence of a fibrous capsule. Quantification of the ectopic bone formation as represented as bone volume (BV) showed a dose response, assessed by micro-CT analysis (Fig. 5*B*).

Evaluation of ABGS in rabbit ulna defect models

The ABC implanted alone did not result in the formation of new bone and failed to achieve rebridgement of the defect (Fig. 6). ABC containing rhBMP6 (ABGS), however, reproducibly induced new bone formation and restored the defect as assessed by radiography. The new bone formation was induced in a dose-dependent manner as represented at weeks 6, 9, 13, 16, 19, and 23 (Fig. 6), and all rabbit ulna are shown at the week 23 (Fig. 7*A*–*C*). Micro-CT analyses showed a dose-dependent increase in bone quantity as examined by bone volume (BV) and medullary volume (MV), which are comparable to the intact bone of the contralateral side (Fig. 7*D*). The bone quality was further confirmed by histology, as shown in a representative sample from each group (Fig. 8). The dose of 100 μg rhBMP6/mL ABC resulted in the complete restoration with fully established cortices and remodeled medullar canal. In three rabbits, a partial synostosis between healed ulna and radius appeared due to the lack of space separating the two bones (Fig. 7*B*). The limitation of the current study is a lack of biomechanical analysis as we have dedicated most of the animals for the radiographic, micro-CT, and histologic analyses.

ABGS versus rhBMP7/bovine collagen

We compared side-by-side rhBMP7/bovine bone collagen device with the ABGS (rhBMP6/ABC) device in the rabbit ulna defect repair model. Collagen alone did not induce bone formation (data not shown), but rhBMP7 containing collagen induced new bone formation (Fig. 9*A*). The rhBMP7/bovine bone collagen commercial device contains 3.5 mg rhBMP7/g of collagen, and to fill the rabbit ulna defect, we used 300 mg that accounts for the total amount of 1.06 mg rhBMP7 in a

collagen carrier. This rhBMP7/collagen-induced rebridgement of the ulna defect was compared with ABGS (100 μg rhBMP6 in 1.5 mL blood) as shown in Fig. 9*A*. ABGS induced, at weeks 2 and 6, a formation of a new uniform bone and underwent a remodeling to rebridge new cortices with adjacent host bone, whereas the bone formation with rhBMP7/collagen was delayed. Micro-CT analysis confirmed that the ABGS containing rhBMP6 induced on week 8 after surgery around 2× more bone volume (Fig. 9*B*, *C*). The differential sensitivity to increasing concentration of Noggin was tested in the C2C12 cell assay, in which rhBMP6 (5 μg) was resistant to Noggin-mediated inhibition compared with rhBMP7 (5 μg) (Fig. 9*D*).

Discussion

Bone morphogenetic proteins have been extensively explored for their remarkable potential to regenerate new bone at ectopic[13] and orthotopic sites.[52] Among BMPs, BMP2 and BMP7 have been used in various clinical studies to promote bone formation both in orthopedic[21,53] and dental[54–56] applications; however, safety issues and limitation in their use were reported.[57–59] The bone devices consisting of a bovine collagen matrix soaked with rhBMP2 or rhBMP7[60,61] were approved by regulatory agencies for the treatment of tibial fractures and nonunions but have also been used off-label for different bone repair indications with an aim to overcome the impaired healing.[61,62]

In the present study, we demonstrate that an autologous bone graft substitute containing rhBMP6 delivered within autologous blood coagulum is capable of inducing new bone formation in rat subcutaneous implants and can rebridge a large segmental defect in ulna of mature rabbits. BMP6 was chosen because it does not bind avidly to Noggin,[63] a natural BMP antagonist abundant in bone and induces downstream

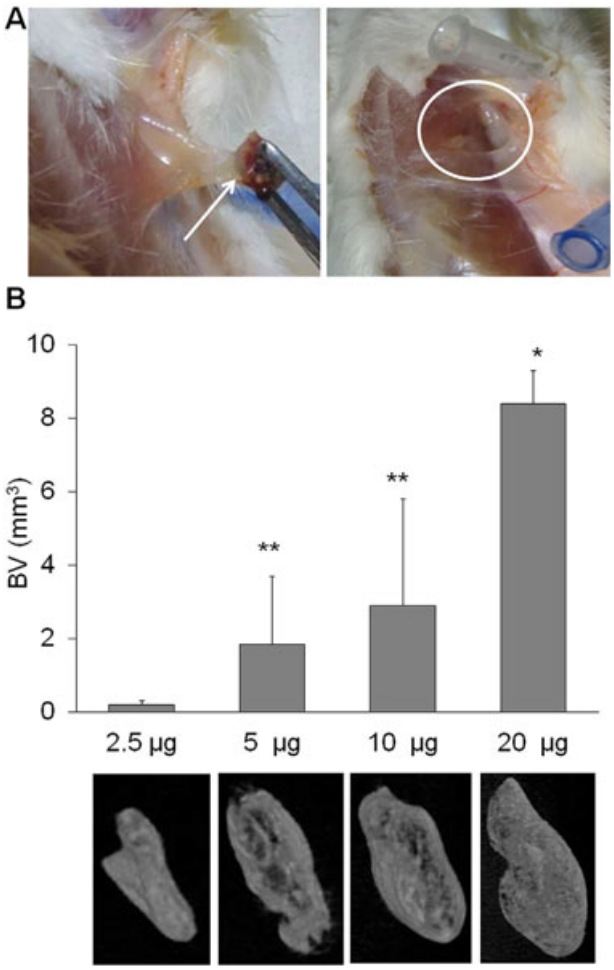

Fig. 5. Rat subcutaneous implants. (*A*) Rat subcutaneous implants in vivo. The white arrow indicates the implant; white circle shows lack of fibrotic tissue accumulation. (*B*) Bone volume (BV) calculated after micro-CT scan in rat subcutaneous implants at day 35 with various rhBMP6 doses and accompanying 3D models of the newly formed bone. The rhBMP6 dose used is represented as μg/implant. Mean ± SEM ($n = 4$ per dose), $^{*}p < 0.01$ versus 2.5 μg, 5 μg, and 10 μg; $^{**}p < 0.05$ versus 2.5 μg.

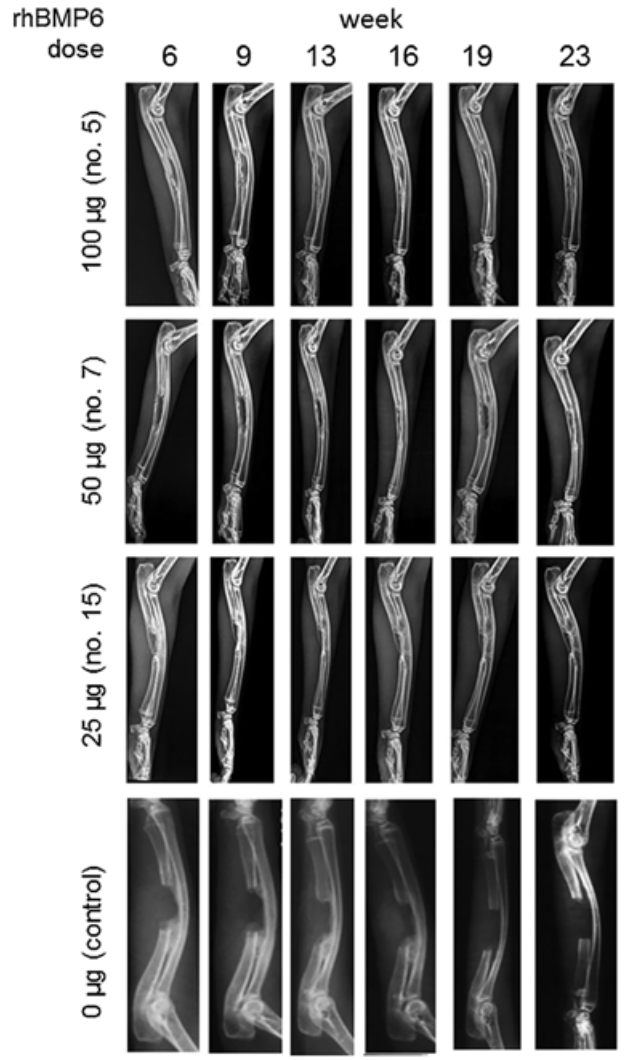

Fig. 6. Radiographs of bone healing through the course of 0 to 23 weeks for different doses of rhBMP6 (0, 25, 50 and 100 μg). Representative rabbit from each treatment group is presented.

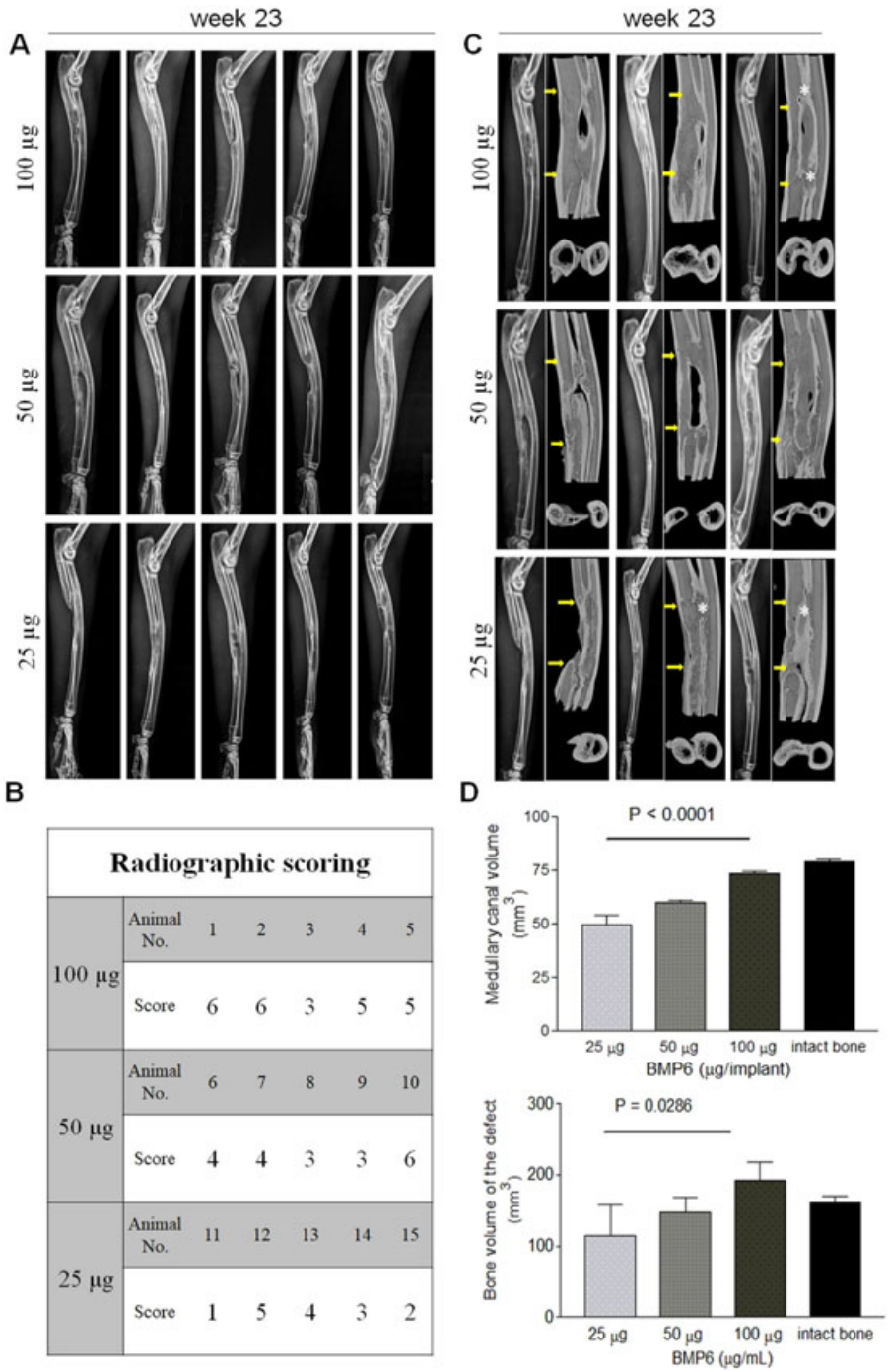

Fig. 7. The effect of rhBMP6 dose on bone healing in rabbit ulna segmental defect. (*A*) Radiographs of all bone samples ($n = 5$ per group) at week 23. (*B*) Radiographic grading scores (0–6) of all bone samples using an established scoring system.[38,39] (*C*) 3D models (longitudinal and cross-sectional) of bone healing in rabbits after ex vivo micro-CT scan at week 23 after study termination. Three bone samples per dose group are shown, with corresponding X-ray image on the left. Yellow arrows indicate initial defect size and introduced bone osteotomy sites. White asterisk indicates a partial synostosis between ulna and radius. (*D*) Quantitative analysis of newly formed bone revealed a dose-dependent manner of rhBMP6 stimulation of bone defect healing. For quantification, the defect site was approximated and delineated manually after which parameters for bone volume (BV) and newly formed endosteal/medullary volume (MV) were calculated. 3D models of the scanned bones were obtained using CTVox (Bruker) software. Quantitative micro-CT parameters were analyzed by one-way ANOVA with post hoc test for linear trend. Each bar represents mean ± SD.

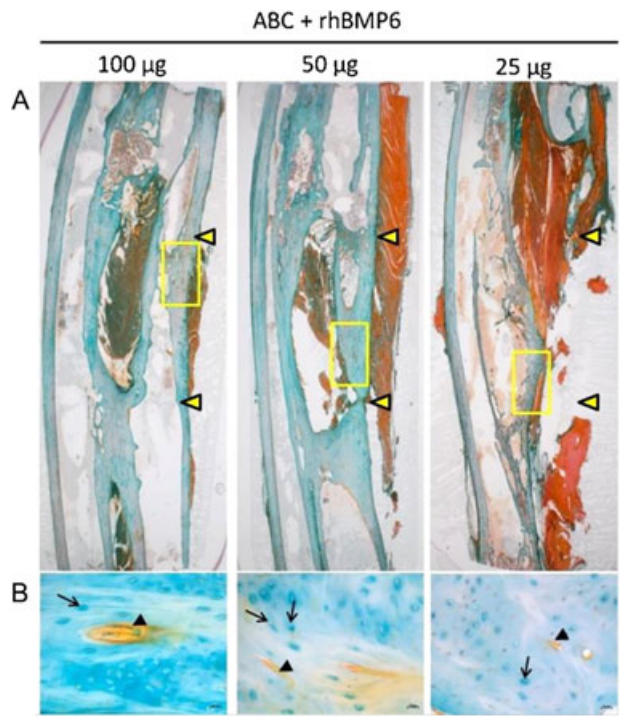

Fig. 8. Evaluation ABGS in ulna critical size defect in rabbits. (*A*) Photomicrographs of histology of representative slides from animals treated with rhBMP6. Rabbits treated with 100 µg rhBMP6 showed a complete restoration with cortical and trabecular bone in the diaphysis and rabbits treated with 50 µg rhBMP6 showed a complete healing with delayed remodeling, while rabbits treated with 25 µg rhBMP6 showed an incomplete rebridgement of bone defect showing a dose-dependent effect at 23 weeks after surgery. Yellow arrowheads denote the size of surgical defects. (*B*) Magnified section of newly formed bone from yellow rectangles in *A*. Black arrowheads indicate blood vessels, and arrows indicate enlarged osteocyte lacunae in the new woven bone under remodeling. Size marker indicates 200 µm.

signaling by spanning across most of the BMP type I and type II receptors that are present on the cell surface of responding osteoprogenitors.[64] These BMP6 biological characteristics support a high specific alkaline phosphatase activity in cultures of established C2C12 mouse cell line[41] and rat osteosarcoma osteoblastic cell line, ROS 17/2.8, compared with other BMPs examined.[63]

A wide range of carriers for BMPs have been investigated for orthopedic indications comprising polymers (synthetic and of natural origin), inorganic materials, and composites ranging from nanoparticles to complex three-dimensional scaffolds, membranes for tissue-guided regeneration, biomimetic surfaces, and smart thermosensitive hydrogels.[65,66] Carrier systems sustain the concentration of the rhBMP at the treatment site, provide temporary scaffolding for osteogenesis, prevent ectopic bone formation, and are ultimately absorbed over time. Autologous blood coagulum was choosen as a preferred scaffold because it provides: 1) fibrin meshwork for rhBMP6 to bind tightly and release it slowly as intact protein over 6 to 8 days; 2) circulating osteoprogenitors for rhBMP6 to respond readily during the fabrication of coagulum; and 3) a permissive environment provoking lesser inflammation and devoid of immune response. In ABGS, most (>95%) of rhBMP6 added to autologous blood bound tightly to plasma proteins in the coagulum, including albumin, thrombin, heparan sulfate, and others. The addition of lower amounts of $CaCl_2$ ensured that the coagulum remains homogeneous, cohesive, syringeable, injectable, and malleable. The time required to achieve the defined physical characteristic of the coagulum appears to be in the range of 45 to 60 minutes. The time to achieve a uniform coagulation of ABC was determined based on the rheological properties (elasticity, stiffness) preferred for injection or implantation to assure a shape at the pocket of segmental defect. This was supported by the coagulum formation over time in human population where 60 minutes provided a safer and more reliable time frame for obtaining implant of desired and necessary quality characteristics (Fig. 2*A*).

In the rat subcutaneous assay, rhBMP6/ABC induces the cascade of cellular events that result in endochondral new bone formation histologically comparable to that of rhBMP2 or rhBMP7 with rat allogenic bone collagen as carrier and/or allogenic DBM[13,67,68] with an accelerated chondrogenesis and osteogenesis as examined at various time intervals after the implantation. The newly formed bone undergoes a typical remodeling that results in ossicles containing functional bone marrow elements with cortices surrounding the implant outerspace and fully maintained the volume of the implant by day 35. The use of ABGS in the subcutaneous assay resulted in absence of inflammation and immune responses compared with animal-derived collagen as shown by a lower neutrophil accumulation and lower total MPO activity.

ABGS (rhBMP6/ABC) induced new bone formation in rabbits and restored ulna critical size defects in a dose-dependant manner, as examined by ex vivo radiographs. The dose of 100 µg/mL ABC induced an optimal bone formation, whereas 25 µg/mL ABC showed a lesser response and at 50 µg/mL of ABC showed an intermediate response. The ABGS-induced bone formation is directly proportional to the dose used and this dose-dependent response is comparable both in rat subcutaneous implants and rabbit ulna segmental defect models, as has previously been shown for rhBMP2 in a gap healing defect canine model.[69] A comparative study with rhBMP7/collagen sponge showed that ABGS induced a new bone that is restricted to the defect area and undergoes remodeling to achieve a complete union quality comparable with native bone. Although preclinical studies have limitations as no given animal model mimics human skeletal and biomechanical conditions in entirety,[39] diaphyseal segmental defect in preclinical studies served as measurable outcome for bone formation toward clinical studies.[70] One of the drawbacks of studies in small animal models (rodents and rabbits) is retaining of notochordal cells in adult life, so the regenerative effect of BMPs may be different from that observed in humans.[21] Another limitation is that four-legged animal loading and precise musculoskeletal structure is mechanically dispositioned compared with humans. The appearance of synostosis between ulna and radius was observed in three rabbits, which reflects the nature of osteogenic BMPs to induce bone formation and fusion upon contact with new and old bone as the space of separation between the ulna and radius is smaller in rabbits than humans.[39]

In summary, we present an ABGS that contains a low dose of rhBMP6 delivered within ABC, a biocompatible native scaffold, and may serve as a safe and robust biological osteoinductive device, which is in contrast to other BMP-based therapies

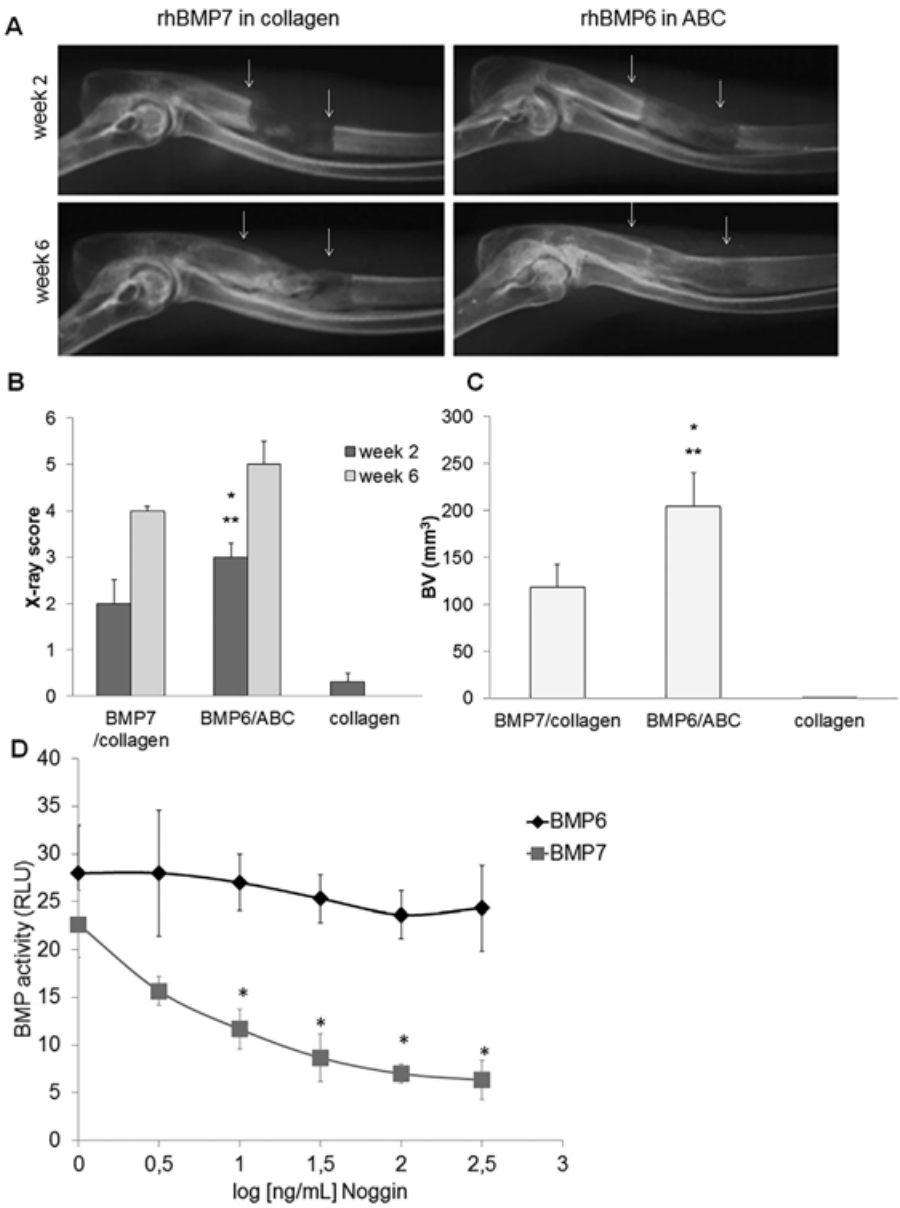

Fig. 9. (*A*) Comparison of rhBMP7/bovine bone collagen with ABGS implant (rhBMP6/ABC) (right) in rabbit ulna segmental defect models at 2 and 6 weeks after administration. (*B*) In vivo X-ray analysis of critical size defects of rabbit ulna 2 and 6 weeks after surgery, treated with 100 μg BMP7 + bovine bone collagen, 100 μg of BMP6 + ABC, and a bovine collagen alone (control) ($n = 8$ rabbits per group). $^{*}p < 0.05$ versus BMP7; $^{**}p < 0.01$ versus control (ANOVA, Dunnett test). (*C*) Ex vivo micro-CT analysis of critical size defects of rabbit ulnas 8 weeks after treatment (the same as in *B*, $n = 8$ per group). $^{*}p < 0.05$ versus BMP7; $^{**}p < 0.01$ versus control (ANOVA, Dunnett test). (*D*) Effects of the inhibitory action of Noggin as examined for BRE-driven luciferase activity in C2C12 cells for BMP6 and BMP7. Each data point is mean ± SD of 3 measured values. $^{*}p < 0.01$ versus BMP6.

(rhBMP2 and rhBMP7), employing bovine Achilles tendon and bone-derived collagen, respectively, and a high BMP dose. More preclinical studies and subsequent evaluation is ongoing,[71] and future clinical trials are needed to address the safety and efficacy of ABGS (rhBMP6/ABC)-based bone graft implant for its potential use in orthopedic patients.

Disclosures

LG, HO and SV have an issued patent US8197840 and licensed to Genera Research (GR). HO received grants and other from GR during the study, RW is a consultant for Pfizer, Stryker, Takeda, Depuy Synthes and Zimmer Biomet, TKS received grants and other from perForm Biologics during the study; SV received grants and other from (GR) and perForm Biologics during the study. Other authors declare no conflict of interest.

Acknowledgments

This program was funded in part by the FP7/2007-2013 program under GA HEALTH-F4-2011-279239 (Osteogrow), by the Horizon 2020 research and innovation program under GA No. 779340

(OSTEOproSPINE), and the Scientific Center of Excellence for Reproductive and Regenerative Medicine (project "Reproductive and regenerative medicine—exploration of new platforms and potentials," GA KK01.1.1.01.0008 funded by the EU through the ERDF).

Authors' roles: Study design: LG, TKS, RW, and SV. Study conduct: LG, MP, IE, MP, TBN, VK, ML, HC, JBS, DM, and HO. Data collection: MP, IE, MP, VK, HC, and MP. Data analysis: LG, MP, IE, TBN, MP, and SV. Data interpretation: IE, MP, HO, RW, and SV. Drafting manuscript: LG, IE, MP, TBN, VK, JBS, RW, and SV. Revising manuscript content: TKS and SV. Approving final version of the manuscript: TKS and SV. SV takes responsibility for the integrity of the data analysis.

References

1. Keating JF, Simpson AH, Robinson CM. The management of fractures with bone loss. J Bone Joint Surg Br. 2005;87(2):142–50.
2. Gubin AV, Borzunov DY, Malkova TA. The Ilizarov paradigm: thirty years with the Ilizarov method, current concerns and future research. Int Orthop. 2013;37(8):1533–9.
3. Sampath K. The systems biology of bone morphogenetic proteins. In: Vukicevic S, Sampath KT, editors. *Bone morphogenetic proteins: systems biology regulators*. Cham, Switzerland: Springer International Publishing; 2017. p. 15–38.
4. Silverman SL, Christiansen C, Genant HK, et al. Efficacy of bazedoxifene in reducing new vertebral fracture risk in postmenopausal women with osteoporosis: results from a 3-year, randomized, placebo-, and active-controlled clinical trial. J Bone Miner Res. 2008;23(12):1923–34.
5. Cummings SR, Ensrud K, Delmas PD, et al. Lasofoxifene in postmenopausal women with osteoporosis. N Engl J Med. 2010; 362(8):686–96.
6. Molina CS, Stinner DJ, Obremskey WT. Treatment of traumatic segmental long-bone defects: a critical analysis review. JBJS Rev. 2014;2(4).
7. Dumic-Cule I, Pecina M, Jelic M, et al. Biological aspects of segmetal bone defects management. Int Orthop. 2015;39(5):1005–11.
8. Einhorn TA. Enhancement of fracture-healing. J Bone Joint Surg 1995;77(6):940–56.
9. Grgurevic L, Erjavec I, Dumic-Cule I, et al. Osteogrow: a novel bone graft substitute for orthopedic reconstruction. In: Vukicevic S, Sampath TK, editors. *Bone morphogenetic proteins: systems biology regulators*. Cham, Switzerland: Springer International Publishing; 2017. p. 215–28.
10. Tong K, Zhong Z, Peng Y, et al. Masquelet technique versus Ilizarov bone transport for reconstruction of lower extremity bone defects following posttraumatic osteomyelitis. Injury. 2017;48(7):1616–22.
11. Kim DH, Rhim R, Li L, et al. Prospective study of iliac crest bone graft harvest site pain and morbidity. Spine J. 2009;9(11):886–92.
12. Schwartz CE, Martha JF, Kowalski P, et al. Prospective evaluation of chronic pain associated with posterior autologous iliac crest bone graft harvest and its effect on postoperative outcome. Health Qual Life Outcomes. 2009;7:49.
13. Reddi AH, Huggins C. Biochemical sequences in the transformation of normal fibroblasts in adolescent rats. Proc Natl Acad Sci U S A. 1972;69(6):1601–5.
14. Vukicevic S, Oppermann H, Verbanac D, et al. The clinical use of bone morphogenetic proteins revisited: a novel biocompatible carrier device OSTEOGROW for bone healing. Int Orthop. 2014;38(3): 635–47.
15. Gazdag AR, Lane JM, Glaser D, Forster RA. Alternatives to autogenous bone graft: efficacy and indications. J Am Acad Orthop Surg. 1995;3(1):1–8.
16. Sampath TK, Reddi AH. Dissociative extraction and reconstitution of extracellular matrix components involved in local bone differentiation. Proc Natl Acad Sci U S A. 1981;78(12):7599–603.
17. Wozney JM, Rosen V, Celeste AJ, et al. Novel regulators of bone formation: molecular clones and activities. Science. 1988;242(4885): 1528–34.
18. Ozkaynak E, Rueger DC, Drier EA, et al. OP-1 cDNA encodes an osteogenic protein in the TGF-beta family. EMBO J. 1990;9(7):2085–93.
19. Micev AJ, Kalainov DM, Soneru AP. Masquelet technique for treatment of segmental bone loss in the upper extremity. J Hand Surg Am. 2015;40(3):593–8.
20. Pecina M, Haspl M, Jelic M, Vukicevic S. Repair of a resistant tibial non-union with a recombinant bone morphogenetic protein-7 (rh-BMP-7). Int Orthop. 2003;27(5):320–1.
21. Giannoudis PV, Kanakaris NK. BMPs in orthopaedic medicine: promises and challenges. In: Vukicevic S, Sampath TK, editors. *Bone morphogenetic proteins: systems biology regulators. Cham*, Switzerland: Springer International Publishing; 2017. p. 187–214.
22. Cook SD, Patron LP, Salkeld SL, Smith KE, Whiting B, Barrack RL. Correlation of computed tomography with histology in the assessment of periprosthetic defect healing. Clin Orthop Relat Res. 2009;467(12):3213–20.
23. Govender S, Csimma C, Genant HK, et al. Recombinant human bone morphogenetic protein-2 for treatment of open tibial fractures: a prospective, controlled, randomized study of four hundred and fifty patients. J Bone Joint Surg Am. 2002;84-A(12):2123–34.
24. Tsiridis E, Morgan EF, Bancroft JM, et al. Effects of OP-1 and PTH in a new experimental model for the study of metaphyseal bone healing. J Orthop Res. 2007;25(9):1193–203.
25. Auregan JC, Begue T. Induced membrane for treatment of critical sized bone defect: a review of experimental and clinical experiences. Int Orthop. 2014;38(9):1971–8.
26. Giannoudis PV, Einhorn TA, Marsh D. Fracture healing: the diamond concept. Injury. 2007;38 Suppl 4:S3–6.
27. Giannoudis PV, Gudipati S, Harwood P, Kanakaris NK. Long bone non-unions treated with the diamond concept: a case series of 64 patients. Injury. 2015;46 Suppl 8:S48–54.
28. Martinovic S, Borovecki F, Miljavac V, et al. Requirement of a bone morphogenetic protein for the maintenance and stimulation of osteoblast differentiation. Arch Histol Cytol. 2006;69(1):23–36.
29. Pecina M, Vukicevic S. Tissue engineering and regenerative orthopaedics (TERO). Int Orthop. 2014;38(9):1757–60.
30. Lissenberg-Thunnissen SN, de Gorter DJ, Sier CF, Schipper IB. Use and efficacy of bone morphogenetic proteins in fracture healing. Int Orthop. 2011;35(9):1271–80.
31. Seeherman HJ, Li XJ, Smith E, Wozney JM. rhBMP-2/calcium phosphate matrix induces bone formation while limiting transient bone resorption in a nonhuman primate core defect model. J Bone Joint Surg Am. 2012;94(19):1765–76.
32. Seeherman HJ, Li XJ, Smith E, Parkington J, Li R, Wozney JM. Intraosseous injection of rhBMP-2/calcium phosphate matrix improves bone structure and strength in the proximal aspect of the femur in chronic ovariectomized nonhuman primates. J Bone Joint Surg Am. 2013;95(1):36–47.
33. Petrauskaite O, Gomes Pde S, Fernandes MH, et al. Biomimetic mineralization on a macroporous cellulose-based matrix for bone regeneration. Biomed Res Int. 2013;2013:452750.
34. Cicciu M, Herford AS, Cicciu D, Tandon R, Maiorana C. Recombinant human bone morphogenetic protein-2 promote and stabilize hard and soft tissue healing for large mandibular new bone reconstruction defects. J Craniofac Surg. 2014;25(3):860–2.
35. Herford AS, Tandon R, Stevens TW, Stoffella E, Cicciu M. Immediate distraction osteogenesis: the sandwich technique in combination with rhBMP-2 for anterior maxillary and mandibular defects. J Craniofac Surg. 2013:24(4):1383–7.
36. Hwang CJ, Vaccaro AR, Lawrence JP, et al. Immunogenicity of bone morphogenetic proteins. J Neurosurg Spine. 2009;10(5):443–51.
37. Aspenberg P, Jeppsson C, Economides AN. The bone morphogenetic proteins antagonist Noggin inhibits membranous ossification. J Bone Miner Res. 2001;16(3):497–500.
38. Benevenia J, Kirchner R, Patterson F, Beebe K, Wirtz DC, Rivero S, et al. Outcomes of a Modular Intercalary Endoprosthesis as Treatment for

Segmental Defects of the Femur, Tibia, and Humerus. Clin Orthop Relat Res. 2016;474(2):539–48.

39. Peric M, Dumic-Cule I, Grcevic D, et al. The rational use of animal models in the evaluation of novel bone regenerative therapies. Bone. 2015;70:73–86.
40. Herrera B, Inman GJ. A rapid and sensitive bioassay for the simultaneous measurement of multiple bone morphogenetic proteins. Identification and quantification of BMP4, BMP6 and BMP9 in bovine and human serum. BMC Cell Biol. 2009;10:20.
41. Paralkar VM, Vukicevic S, Reddi AH. Transforming growth factor beta type 1 binds to collagen IV of basement membrane matrix: implications for development. Dev Biol. 1991;143(2):303–8.
42. Simic P, Buljan Culej J, Orlic I, et al. Systemically administered bone morphogenetic protein-6 restores bone in aged ovariectomized rats by increasing bone formation and suppressing bone resorption. J Biol Chem. 2006;281(35):25509–21.
43. Vukicevic S, Sampath TK, editors. *Bone morphogenetic proteins: systems biology regulators*. Cham, Switzerland: Springer International Publishing; 2017.
44. Vukicevic S, Basic V, Rogic D, et al. Osteogenic protein-1 (bone morphogenetic protein-7) reduces severity of injury after ischemic acute renal failure in rat. J Clin Invest. 1998;102(1):202–14.
45. Grgurevic L, Macek B, Mercep M, et al. Bone morphogenetic protein (BMP)1-3 enhances bone repair. Biochem Biophys Res Commun. 2011;408(1):25–31.
46. Cook SD, Baffes GC, Wolfe MW, Sampath TK, Rueger DC. Recombinant human bone morphogenetic protein-7 induces healing in a canine long-bone segmental defect model. Clin Orthop Relat Res. 1994(301):302–12.
47. Paralkar VM, Borovecki F, Ke HZ, et al. An EP2 receptor-selective prostaglandin E2 agonist induces bone healing. Proc Natl Acad Sci U S A. 2003;100(11):6736–40.
48. Erjavec I, Bordukalo-Niksic T, Brkljacic J, et al. Constitutively elevated blood serotonin is associated with bone loss and type 2 diabetes in rats. PLoS One. 2016;11(2):e0150102.
49. Sampath TK, Simic P, Sendak R, et al. Thyroid-stimulating hormone restores bone volume, microarchitecture, and strength in aged ovariectomized rats. J Bone Miner Res. 2007;22(6):849–59.
50. Vukicevic S, Krempien B, Stavljenic A. Effects of 1 alpha,25- and 24R,25-dihydroxyvitamin D3 on aluminum-induced rickets in growing uremic rats. J Bone Miner Res. 1987;2(6):533–45.
51. Krempien B, Vukicevic S, Vogel M, Stavljenic A, Buchele R. Cellular basis of inflammation-induced osteopenia in growing rats. J Bone Miner Res. 1988;3(5):573–82.
52. Urist MR. Bone: formation by autoinduction. Science. 1965; 150(3698):893–9.
53. Vukicevic S, Grgurevic L, Pecina M. Clinical need for bone morphogenetic proteins. Int Orthop. 2017;41(11):2415–16.
54. Cicciu M, Herford AS, Juodžbalys G, Stofella E. Recombinant human bone morphogenetic protein type 2 application for a possible treatment of bisphosphonates-related osteonecrosis of the jaw. J Craniofac Surg. 2012;23(3):784–8.
55. Herford AS, Cicciu M. Recombinant human bone morphogenetic protein type 2 jaw reconstruction in patients affected by giant cell tumor. J Craniofac Surg. 2010;21(6):1970–5.
56. Herford AS, Cicciu M, Eftimie LF, et al. rhBMP-2 applied as support of distraction osteogenesis: a split-mouth histological study over nonhuman primates mandibles. Int J Clin Exp Med. 2016;9(9): 17187–94.
57. Fu R, Selph S, McDonagh M, et al. Effectiveness and harms of recombinant human bone morphogenetic protein-2 in spine fusion: a systematic review and meta-analysis. Ann Intern Med. 2013; 158(12):890–902.
58. Simmonds MC, Brown JV, Heirs MK, et al. Safety and effectiveness of recombinant human bone morphogenetic protein-2 for spinal fusion: a meta-analysis of individual-participant data. Ann Intern Med. 2013;158(12):877–89.
59. Cicciù M. Real opportunity for the present and a forward step for the future of bone tissue engineering. J Craniofac Surg. 2017;28(3): 592–3.
60. Bishop GB, Einhorn TA. Current and future clinical applications of bone morphogenetic proteins in orthopaedic trauma surgery. Int Orthop. 2007;31(6):721–7.
61. White AP, Vaccaro AR, Hall JA, Whang PG, Friel BC, McKee MD. Clinical applications of BMP-7/OP-1 in fractures, nonunions and spinal fusion. Int Orthop. 2007;31(6):735–41.
62. Pradhan BB, Bae HW, Dawson EG, Patel VV, Delamarter RB. Graft resorption with the use of bone morphogenetic protein: lessons from anterior lumbar interbody fusion using femoral ring allografts and recombinant human bone morphogenetic protein-2. Spine (Phila PA 1976). 2006;31(10):E277–84.
63. Song K, Krause C, Shi S, et al. Identification of a key residue mediating bone morphogenetic protein (BMP)-6 resistance to noggin inhibition allows for engineered BMPs with superior agonist activity. J Biol Chem. 2010;285(16):12169–80.
64. Ebisawa T, Tada K, Kitajima I, et al. Characterization of bone morphogenetic protein-6 signaling pathways in osteoblast differentiation. J Cell Sci. 1999;112 (Pt 20):3519–27.
65. Stylios G, Wan T, Giannoudis P. Present status and future potential of enhancing bone healing using nanotechnology. Injury. 2007;38 Suppl 1:S63–74.
66. Begam H, Nandi SK, Kundu B, Chanda A. Strategies for delivering bone morphogenetic protein for bone healing. Mater Sci Eng C Mater Biol Appl. 2017;70(1):856–69.
67. Sampath TK, Maliakal JC, Hauschka PV, et al. Recombinant human osteogenic protein-1 (hOP-1) induces new bone formation in vivo with a specific activity comparable with natural bovine osteogenic protein and stimulates osteoblast proliferation and differentiation in vitro. J Biol Chem. 1992;267(28):20352–62.
68. Wang EA, Rosen V, D'Alessandro JS, et al. Recombinant human bone morphogenetic protein induces bone formation. Proc Natl Acad Sci U S A. 1990;87(6):2220–4.
69. Sumner DR, Turner TM, Urban RM, Turek T, Seeherman H, Wozney JM. Locally delivered rhBMP-2 enhances bone ingrowth and gap healing in a canine model. J Orthop Res. 2004;22(1):58–65.
70. Vukicevic S, Sampath TK, editors. *Bone morphogenetic proteins: from laboratory to clinical practice*. Basel: Birkhauser Verlag; 2002.
71. European Medicines Agency. EU clinical trials register [Internet]. Available at: https://www.clinicaltrialsregister.eu/.